A NEW STEREO CORRESPONDENCE METHOD FOR SNAKE-BASED OBJECT SEGMENTATION

Ashraf M. Alattar and Jong Whan Jang

Department of Information and Communication Engineering, PaiChai University
Daejeon, South Korea
{ashraf, jangjw}@pcu.ac.kr

ABSTRACT

In this paper, we propose a new method for generating excellent external energy for snake-based object segmentation methods in stereo images. Our method first generates an edge-based disparity map by performing stereo correspondence between multi-level edge maps of the stereo image pair. Only edges of similar strength are considered for matching. To filter the disparity map for edges of the object of interest, the method estimates the object's disparity value by matching the pattern of edges of the region of interest in the left image against candidate patterns in the right image. The filtered edge map is then used to generate external energy for the snake. The proposed method has been tested on two snake models and results show a noticeable enhancement on performance of the snake when compared with other methods.

Index Terms— Snake, segmentation, stereo, edge maps, disparity

1. INTRODUCTION

Active contour (snake) models for monocular images have been extensively studied and used in many applications such as facial image processing [6,9], object tracking [1,4] and medical imaging [2,8]. However, the performance of snake models degrades significantly when they encounter challenges such as boundary concavities, object occlusion, and background noise and clutter. Recently, snake-based segmentation methods have been revitalized with the advent of stereo and multi-view imaging technology. An increasing volume of research effort has been focused on combining depth information with snake-based segmentation. This depth information can be easily extracted from multiple views of the object.

In [5] Kim et al. proposed a new snake-based algorithm for object segmentation in stereo images. This algorithm first calculates a disparity map using a region-based stereo matching technique. It then uses this disparity map to compute the external energy term of the snake. Given an object of interest (OOI), to estimate its disparity value (D_{OOI}), Kim's algorithm calculates a disparity histogram of the region of interest (ROI), then it takes its peak to indicate D_{OOI}. This method generally works, but it fails when the objects have thin and curved shapes. These objects do not fill up the ROI and hence cause the failure. In this paper we take a different approach than Kim's for generating the external energy and estimating the OOI's disparity value. We propose to generate the external energy using edge-based rather than region-based stereo matching. Our algorithm creates a multi-level edge map of each image in the stereo pair and performs stereo matching under the constraint of edge strength similarity. The strength similarity constraint decreases matching errors and reduces the search space, which makes our proposed algorithm faster and the generated result more accurate.

To estimate the OOI's depth, our method relies on finding the displacement at which a best match of the object's significant edges is found on the right image. The search uses a correlation measure, and results in a more accurate estimation of the object's depth, which plays a clear role in enhancing the overall segmentation performance.

This paper is organized in four sections in addition to the introduction. The next section presents some essentials on snake-based object segmentation. Section 3 details the main aspects of our new method for extracting edges of the object of interest. Section 4 presents an evaluation of the proposed method. It includes experimental results using two snake models, and Section 5 presents some conclusions.

2. SNAKE-BASED OBJECT SEGMENTATION

An Active Contour (Snake) is an energy minimizing model guided by internal constraint forces and influenced by external forces which attract it toward features such as lines and edges. In snake-based object segmentation methods, snakes are iteratively attracted to the OOI until they converge to its boundary. Snake models are broadly classified into parametric and geometric. The parametric snake model was first introduced by Kass et al. in [4] as an energy minimizing spline. In its discrete formulation, a parametric snake is a set of points $v_i = (x_i, y_i)$ for $i = 0, \dots, M-1$ where x_i and y_i are the x and y coordinates of the snake point respectively, and M is the total number of snake points. The energy model for the parametric snake is a functional that is typically written as:

$$E_{snake} = \sum_{i=0}^{M-1} \left(E_{int}(v_i) + E_{ext}(v_i) \right) \quad (1)$$

The E_{int} energy term is called the internal energy term, and it is concerned with snake properties such as bending and discontinuity. E_{ext} is the external energy term and it is usually defined as the gradient of the intensity image.

A major shortcoming of parametric snakes is their inability to proceed into boundary concavities. Some research solutions have been proposed to handle this problem such as the gradient vector flow (GVF) snake proposed by Xu et al. in [10], and our previous work reported in [4].

A geometric active contour, also known as geodesic active contour (GAC), is formulated as a curve C that has a weighted length $L_g(C)$ such that:

$$L_g(C) = \int_0^1 g\big(C(p)\big)|C'(p)|dp, \quad (2)$$

where g refers to image forces and is defined, similarly to the parametric snake model, in terms of the image gradient as $g = 1/(1 + |\nabla \mathrm{G}_\sigma * \mathrm{I}|^2)$. GAC snakes seek to minimize their total weighted length by solving the gradient flow equation:

$$\frac{\partial C}{\partial t} = gkN - \langle \nabla g, N \rangle N \quad (3)$$

where k is curvature force, N is the normal vector, and $\langle , \rangle$ is the inner product. The second term of the right-hand-side of equation (3) represents the external energy for the GAC. GAC snakes are typically implemented using level set techniques where they are embedded as the zero level set of a higher dimensional function, see [7]. This implementation enables GAC snakes to handle boundary concavities and topology changes naturally.

3. NEW OBJECT SEGMENTATION METHOD

Our new method for object segmentation in stereo images derives disparity information from the stereo image pair by a new stereo matching technique and exploits this information to produce a filtered edge map containing only edges of the OOI. This edge map is then used for generating external energy for snakes. Given a manually defined ROI around the OOI, this method generates an edge map of the object of interest isolated from background edges.

3.1. Multi-level edge maps

The primary element of our new method is to build two multi-level edge maps one for the left and another for the right image. The edges are classified based on their strength into one of four levels. The set $Q = \{q | q \in 1, \dots, 4\}$ represents the four edge strength levels: $Very\ Weak\ (VW)$, $Weak\ (W)$, $Medium\ (M)$, and $Strong\ (S)$, respectively. This classification of edges is essential for the stereo matching step as will be explained in Section 3.3. To create the four-level classified edge maps any of the common edge operators can be used. For this purpose a set of four monotonically increasing thresholds $\{Th_q\}$ is used. Th_1 is set to 0. In our work, we used the Canny edge operator. The final edge map, $L(x, y)$, is the summation of the four edge maps, $L_q(x, y)$, produced at each of the four thresholds; i.e. $L(x, y) = \sum_{q=1}^{4} L_q(x, y)$. This classification of edges serves to control the matching process in a way where only edges of similar strength are matched. This scheme improves matching quality and speed by avoiding unlikely matches. Figure 1 shows the multi-level edge maps of two corresponding left and right ROIs.

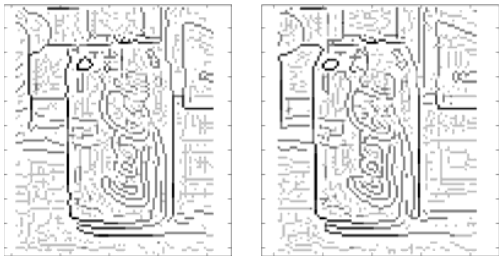

Figure 1: Multi-level edge maps, left & right respectively

3.2. Estimation of the OOI's disparity by target localization

Estimating the OOI's disparity is a first step that is vital for all other proceeding steps. In [5] Kim et al. estimated the disparity of the OOI based on the peak of a disparity histogram of pixels in the region enclosed by the snake. Kim's method assumes that the disparity map is dense and the object covers most of the snake region. In this paper, both of those conditions are not required since the disparity map is edge-based. The objects are allowed to have thin curved shapes or occupy a small area of the snake region (see Figure 2).

The method in this paper effectively handles these assumptions by adopting a target localization approach. A correlation-based similarity search is used to find the best

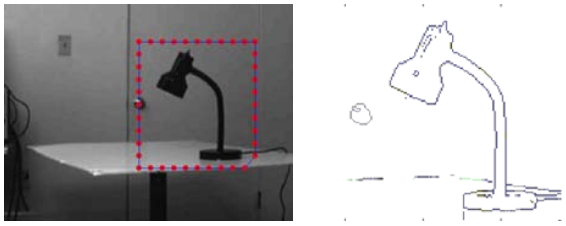

Figure 2: Thin curved object and its edge-based disparity map

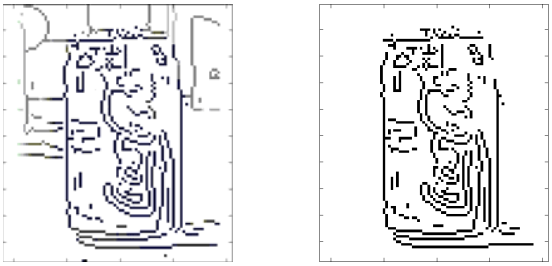

Figure 3: Edge disparity map (left), and $LEDM$ (right)

match between edges inside the ROI in the left image and those in the right image. This search is limited to edges of the significant levels (W, M, S) only. For n such edge pixels in the ROI, let $\{(x_i, y_i)\}_{i=1\ldots n}$ be the set of their pixel locations, let x_0 be the x-coordinate of the center of ROI, and u be the x displacement starting at x_0. The Sum of Squared Differences (SSD) correlation measure is used to estimate the similarity between edges in the ROI and candidate edge patterns in the right image as defined bellow:

$$S(u) = \sum_{i=1}^{n} \big(L_l(x_i,\, y_i) - L_r(x_i + u,\, y_i)\big)^2 \qquad (4)$$

where L_l and L_r are the left and right multi-level edge maps, respectively. The x displacement which scores the best correlation determines the best estimate for D_{OOI}.

3.3. Stereo matching

The stereo correspondence process is significantly improved with the proposed classification of edge pixels since only pixels of similar strength are matched. Excluding $Very\,Weak$ edges, which are of no significance to the stereo matching process, stereo matching is performed on $Strong$, $Medium$, and $Weak$ edges only. Since edge strength may differ between the left and right images, the similarity constraint is relaxed. The similarity constraint is imposed on $Strong$ and $Weak$ edges only. This is because a $Weak$ edge in one image is very unlikely to appear as a $Strong$ edge in the other image, and vice versa. Any correlation method may be used for the stereo matching. In our work the Sum of Absolute Differences (SAD) method produced adequate results.

The matching process also uses a matching technique with a variable window size that depends on edge strength. Since weak edges are typically located within low-textured regions, it is reasonable to expect their correspondence results to be less reliable when a matching window of small size is used. Therefore, we used three window sizes (3×3, 5×5, and 7×7) in inverse proportion to edge strength.

Furthermore, to improve the quality of the output disparity map, we adopted a two-phase stereo matching technique. The aforementioned matching process is followed by a second phase that uses a wider window size to re-match any no-matches which may have resulted in the first phase. Figure 3 (left) shows an example edge-based disparity map produced using our stereo matching method.

3.4. External energy formulation

In the final step, the edge-based disparity map is filtered to yield an edge map of edges belonging to only the OOI. To handle cases of objects with varying disparity values across their surface, we allow a tolerance factor, ε, in the filtering procedure. We call the resulting edge map a layer edge disparity map ($LEDM$), and it is defined as follows:

$$f_{LEDM}(x,y) = \begin{cases} 1, & |D_{OOI} - D(x,y)|/D_{OOI} < \varepsilon \\ 0, & otherwise \end{cases} \qquad (5)$$

where $D(x,y)$ is the disparity map and D_{OOI} is the object's disparity. The edge map shown in Figure 3 (right) is an example $LEDM$. Further processing of the $LEDM$ map depends on the particular snake model to be used for segmentation. This includes the generation of a gradient map, as in the case of most snake methods, or the generation of a gradient field, as in the case of the GVF snake.

4. EXPERIMENTAL RESULTS

We have implemented our new stereo correspondence method and evaluated its performance using two snake models: the GVF Snake, and the GAC Snake. A set of four test images was used for each snake model and the root mean square error (RMSE) was used to compare the performance. The RMSE measure calculates the root of the mean error between a manually defined correct contour and the final contour calculated by the model, and is defined as:

$$RMSE = \sqrt{\frac{\sum_{i=1}^{M} \|v_i - o_i\|^2}{M}} \qquad (6)$$

where v_i is a snake point in the final snake contour, o_i is the nearest point in the true contour, and M is the number of snake points.

We implemented our proposed stereo correspondence method using MATLAB and ran the experiments on a Pentium 4 machine with 1 GB RAM and a 2.8 GHz clock speed. A set of four images having a 320×240 resolution was used to test the method, and the set of thresholds $\{0.0, 0.1, 0.45, 0.75\}$ was used for generating the multi-level edge maps.

Columns (a)-(c) in Figure 4 show the results of applying our method to each of the four test images. For each test image, column (a) shows the manually-defined ROI, column (b) shows the generated edge-based disparity map, and column (c) shows the final $LEDM$ containing only the object's edges. These results show that the proposed method has successfully estimated the object's disparity and

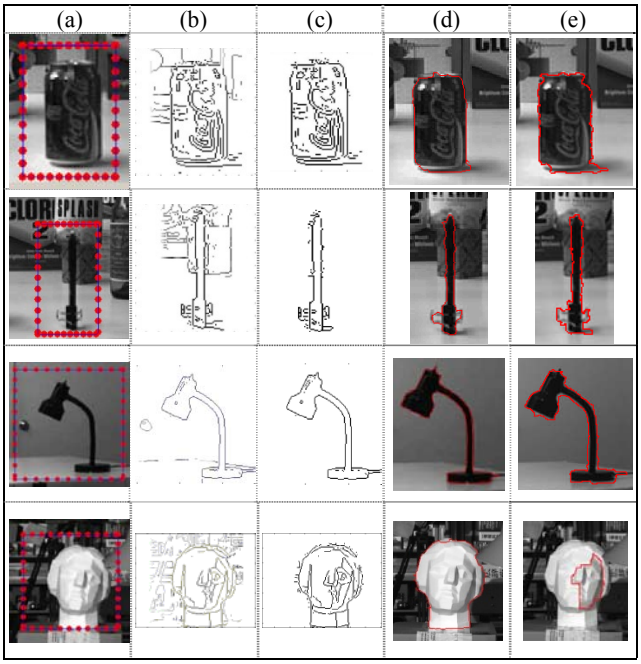

Figure 4: Method results: (a) ROI, (b) edge-based disparity map, (c) LEDM, (d, e) Segmentation results for GVF and GAC snakes, respectively.

eliminated most of the foreign edges which belong to noise and/or surrounding background.

Columns (d) and (e) in Figure 4 show the results from extracting the objects of interest using the two snake models: the GVF snake, (d), and the GAC snake, (e). For both snake models, external energy was generated based on each object's *LEDM* (shown in column c). Performance of the two snake models varied primarily according to the way each model handles boundary concavities. While it is always desirable to penetrate and converge to boundary concavities, it was not desirable in some cases to do so in very narrow boundary gaps which have resulted from faded or very weak edges of the boundary. As can be seen in Figure 4-e, these gaps caused the GAC snake to "break loose" inside and eventually miss the object completely. This is due to the GAC model's high sensitivity to boundary continuity. The GVF model, however, maintained an acceptable degree of rigidity while at the same time penetrating boundary concavity, and thus, gave better results. Table 1 gives a comparison of performance for both of the snake models measured in terms of RMSE on each of the test objects.

5. CONCLUSION

Experiments show that the new method produced cleaner external energy for active contour models, and unlike other snake-based segmentation methods, it is not sensitive to snake point initialization. Obstacles, such as object occlusion and background noise and clutter, which usually degrade performance of snake models, are significantly reduced. Limiting the stereo matching to edges of similar strength has significantly decreased processing time required to generate the edge map compared with other edge-based stereo matching methods. Furthermore, the new stereo matching method relieves snake methods from calculating useless external energy related to foreign edges (particularly in the case of GVF snakes where calculation of the GVF field consumes a major portion of processing time). Performance of the two tested snake models was strongly influenced by their handling of boundary concavities and gaps. In future research we intend to consider ways for eliminating boundary gaps which may appear in edge maps of objects with faded or very weak boundary segments.

Table 1: RMSE values for snakes on the test objects

	Can	Pen	Lamb	Tsukuba
GVF	2.4	2.5	1.8	2.8
GAC	4.3	4.4	3.5	8.5

6. REFERENCES

[1] Couvignou, P. A., N. P. Papanikolopoulos, and P. K. Khosla. "On the use of snakes for 3-D robotic visual tracking," *IEEE CVPR* 1993, pp. 750-751, June 1993.

[2] Fok, Y. L., J. C. K. Chan, and R. T. Chin. "Automated analysis of nerve-cell images using active contour models," *IEEE Trans. Med. Imag.,* vol. 15, no. 3, pp. 353-368, June 1996.

[3] Kass, M., A. Witkin, and D. Terzopoulos. "Snake: Active Contour Models." *Int'l J. Computer Vision,* vol. 1, no. 4, pp. 321-331, 1987.

[4] Kim, S. H., A. M. Alattar, and J. W. Jang. "Snake-Based Object Tracking in Stereo Sequences with the Optimization of the Number of Snake Points," *ICIP 2006,* pp. 193-196, Oct. 2006.

[5] Kim, S. H., J. W. Jang, and J. H. Choi. "Object Segmentation Algorithm Using Snakes in Stereo Images," *Optical Engineering,* vol. 45, no. 3, pp. 037005, Mar. 2006.

[6] Lam, K. M., and H. Yan. "Fast algorithm for locating head boundaries," *J. Elec. Imag.,* vol. 3, no. 4, pp. 351-359, Oct. 1994.

[7] Malladi, R., J. A. Sethian, and B. C. Vemuri. "Shape modeling with front propagation: A level set approach," *IEEE Trans. Pat. Anal. Mach. Intell.,* vol. 17, no. 2, pp. 158-175, June 1995.

[8] McInernery, T., and D. Terzopolous. "Deformable models in medical image analysis: A survey," *Med. Imag. Anal.*, vol. 1, no. 2, pp. 91-108, 1996.

[9] Waite, J. B., and W. J. Welsh. "Head boundary location using snakes," *Brit. Telecom Tech. J.,* vol. 8, no. 3 pp. 127-135, 1990.

[10] Xu, Chenyang, and Jerry L. Prince. "Snakes, Shapes, and Gradient Vector Flow," *IEEE Transactions on Image Processing,* vol. 7, no. 3, pp. 359-369, March 1998.